

Solutions to the relativistic precession model

Adam Ingram^{1*} & Sara Motta²

¹*Astronomical Institute, Anton , University of Amsterdam, Science Park 904, 1098 XH Amsterdam, the Netherlands.*

²*ESAC, European Space Astronomy Centre, Villanueva de la Cañada, E-28692 Madrid, Spain*

Accepted 2014 August 4. Received 2014 July 4; in original form 2014 July 4

ABSTRACT

The relativistic precession model (RPM) can be used to obtain a precise measurement of the mass and spin of a black hole when the appropriate set of quasi periodic oscillations is detected in the power-density spectrum of an accreting black hole. However, in previous studies the solution of the RPM equations could be obtained only through numerical methods at a price of an intensive computational effort. Here we demonstrate that the RPM system of equations can be solved analytically, drastically reducing the computational load, now limited to the Monte-Carlo simulation necessary to estimate the uncertainties. The analytical method not only provides an easy solution to the RPM system when three oscillations are detected, but in all the cases where the detection of two simultaneous oscillations is coupled with an independent mass measurement. We also present a computationally inexpensive method to place limits on the black hole mass and spin when only two oscillations are observed.

Key words: Black hole physics; X-rays: binaries; X-rays: individual: GRO J1655-40, XTE J1550-564, H 1743-322

1 INTRODUCTION

Quasi periodic oscillations (QPOs) were discovered several decades ago in the X-ray flux of accreting stellar mass black holes (BHs) and neutron stars (NSs). It is now clear that QPOs are a common characteristic of accreting systems, having also been observed from *Ultra Luminous X-ray sources* (Strohmayer et al. 2003) and, for a few cases, Active Galactic Nuclei (AGN, Gierliński et al. 2008). QPOs take the form of narrow peaks in the Fourier power spectrum of the X-ray light curve, and thus their centroid frequencies can be measured with high accuracy, offering the opportunity to accurately probe the distorted spacetime in the vicinity of a compact object. From their short timescales and high coherence, simple light crossing arguments indicate that these phenomena must originate from the innermost regions of the accretion flow.

In spite of being studied extensively since their discovery, the physical origin of QPOs remains ambiguous. However, years of comprehensive monitoring by the Rossi X-ray Timing Explorer (*RXTE*) has yielded a detailed phenomenological knowledge of QPO observational properties. In BH X-ray binaries, low frequency QPOs (LF QPOs) are very strong and commonly observed features and have been split up into three subclasses: Type-A, B and C (see e.g. Wijnands et al. 1999, Casella et al. 2005, Motta et al. 2012). Type-C QPOs are by far the most commonly observed. Their centroid frequency usually varies in the ~ 0.1 –30 Hz range and tightly correlates with the spectral evolution of the host source (see e.g.

Belloni et al. 2011). Pairs of high frequency QPOs (HF QPOs), with centroid frequencies $\gtrsim 100$ Hz, have also been observed, even though they are much harder to detect above the Poisson noise level. Nonetheless, they have sparked much theoretical interest because their frequencies are commensurate with the orbital frequency close to the BH (see e.g. Abramowicz & Kluźniak 2001, Kluźniak & Abramowicz 2001, Lamb & Miller 2001). LF QPOs are also observed in NS X-ray binaries with higher centroid frequencies, consistently with linear mass scaling. The NS analogy to HF QPOs are kHz QPOs which, in contrast to their BH counterparts, are regularly observed, often with very high amplitude (van der Klis 1996).

There are many suggested QPO mechanisms in the literature that can be divided into two main groups: those associated to wave modes of the accretion flow (Tagger & Pellat 1999, Titarchuk & Osherovich 1999, Wagoner et al. 2001, Cabanac et al. 2010), and those associated with relativistic effects that involve the misalignment of the accretion flow and the black hole spin (Stella & Vietri 1998, Lamb & Miller 2001, Abramowicz & Kluźniak 2001, Fragile et al. 2005, Schnittman et al. 2006, Homan et al. 2006, Ingram & Done 2011). This second group of models are based on the idea that, whereas in Newtonian gravity bound elliptical orbits around a point-like gravitating mass always remain in the same plane with a stationary semi-major axis, in the theory of General Relativity (GR) this is not the case. Mathematically, this means that the three coordinate frequencies: orbital, vertical and radial epicyclic are not equal, $\nu_\phi \neq \nu_\theta \neq \nu_r$. Periastron precession, with frequency

* E-mail: a.r.ingram@uva.nl

$\nu_{\text{per}} = \nu_{\phi} - \nu_r$ is a precession of an elliptical orbit's semi-major axis. Nodal (Lense-Thirring) precession, which occurs only for orbits out of the equatorial plane of a spinning gravitating mass, is a precession of the orbit's spin axis around the spin axis of the gravitating mass. This has a frequency $\nu_{\text{nod}} = \nu_{\phi} - \nu_{\theta}$. All of these frequencies depend only on the radius of the orbit, r , and the mass, M , and dimensionless spin parameter, $-1 < a < 1$, of the gravitating mass.

In the relativistic precession model (RPM) proposed by Stella & Vietri 1998, the Type-C QPO originates from nodal precession, the lower HF QPO from periastron precession and the upper HF QPO from orbital motion, with all three signals originating from one characteristic radius, r . The inward movement of this radius can then explain the observed co-evolution of the three QPOs to higher frequencies (e.g. Stella et al. 1999). This model has been applied with mixed success to NSs (Stella & Vietri 1999; Ingram & Done 2010; Altamirano et al. 2012), but appears to work very well for BHs. In particular, Motta et al. (2014; hereafter M14) considered an observation of GRO 1655-40 in which the presence of three simultaneously observed QPOs leaves three equations and three unknowns. They were thus able to solve the equations of the RPM to obtain values of r , a and M . Encouragingly, they found that the mass measured in this way agrees very well with the dynamical mass measurement for this source (Beer & Podsiadlowski 2002). Unfortunately, the simultaneous occurrence of the three QPOs relevant for the RPM is extremely rare and so it is not possible to simply apply this technique to every BH. However, a spin measurement can be achieved also in the case where the mass of the BH is known and two simultaneous QPOs are detected, as suggested by Motta et al (2014a; hereafter M14a).

In previous studies, the equations of the RPM have been solved numerically in a very computationally intensive manner (M14; M14a; Bambi et al. 2014; Stefanov 2014), resulting from a belief that the equations cannot be solved analytically. Here, we present an analytic solution for the case where three QPOs are detected. We also present simple methods to solve for all occurrences where two QPO detections are combined with a mass measurement. Although we could not find an entirely analytic solution for the latter case, our method is far quicker than all previously used methods. In addition we consider a method to place tight limits on system parameters with only two QPOs and no mass measurement.

2 SOLVING THE SYSTEM WITH THREE QPOs

In the case of a test mass orbiting a spinning BH in a plane slightly perturbed from equatorial, it can be shown that, in Kerr metric (Bardeen et al. 1972; Merloni et al. 1999), the orbital, periastron precession and nodal precession frequencies are given by:

$$\nu_{\phi} = \pm \frac{\beta}{M} \frac{1}{r^{3/2} \pm a} \quad (1)$$

$$\nu_{\text{per}} = \nu_{\phi} \left[1 - \sqrt{1 - \frac{6}{r} \pm \frac{8a}{r^{3/2}} - \frac{3a^2}{r^2}} \right] \quad (2)$$

$$\nu_{\text{nod}} = \nu_{\phi} \left[1 - \sqrt{1 \mp \frac{4a}{r^{3/2}} + \frac{3a^2}{r^2}} \right], \quad (3)$$

where M is BH mass in units of solar masses, r is radius in units of $R_g = GM_{\odot}/c^2$, a is the dimensionless spin parameter and $\beta = c^3/(2\pi GM_{\odot}) = 3.237 \times 10^4$ Hz. In all equations, the top

sign refers to prograde spin (i.e. orbital motion is in the same direction as BH spin) and the bottom sign refers to retrograde spin. Since no stable orbits exist inside of the innermost stable circular orbit (ISCO), we can set the extra condition $r > r_{\text{ISCO}}$. The radius r_{ISCO} depends monotonically on the spin (see Bardeen et al. 1972; M14), ranging from $9 > r_{\text{ISCO}} > 1$ for $-1 < a < 1$ and taking the value $r_{\text{ISCO}} = 6$ for $a = 0$.

In the RPM, $\nu_{\text{LF}} = |\nu_{\text{nod}}|$, $\nu_l = |\nu_{\text{per}}|$ and $\nu_u = |\nu_{\phi}|$, where ν_{LF} , ν_l and ν_u are respectively the measured Type-C, lower HF and upper HF QPO frequencies (M14). The equations of the RPM depend on the mass and the spin of the compact object, on the radius at which the frequencies are produced and on the frequencies themselves. If we have measurements of all three QPO frequencies simultaneously, we can solve for the three remaining unknowns (mass, spin and emission radius), assuming that all the frequencies are associated with the same radius.

We see that the mass is explicitly contained only in equation 1 and so the equations for ν_{per} and ν_{nod} form a system of two simultaneous equations which we can solve to get r and a before calculating M from equation 1. Re-arranging equations 2 and 3 gives:

$$\Gamma \equiv \left(1 - \frac{\nu_{\text{per}}}{\nu_{\phi}} \right)^2 = 1 - \frac{6}{r} \pm \frac{8a}{r^{3/2}} - \frac{3a^2}{r^2} \quad (4)$$

$$\Delta \equiv \left(1 - \frac{\nu_{\text{nod}}}{\nu_{\phi}} \right)^2 = 1 \mp \frac{4a}{r^{3/2}} + \frac{3a^2}{r^2}. \quad (5)$$

For $r > r_{\text{ISCO}}$, these constants obey $0 < \Delta < 1$, $0 < \Gamma < 1$, and $\Delta > \Gamma$. Adding together equations 4 and 5 gives a in terms of r :

$$a = \pm \frac{r^{3/2}}{4} \left[\Delta + \Gamma - 2 + \frac{6}{r} \right]. \quad (6)$$

Taking twice equation 5 and adding it to 4 gives:

$$3 - 2\Delta - \Gamma - \frac{6}{r} + \frac{3a^2}{r^2} = 0. \quad (7)$$

Substituting equation 6 into 7 and re-arranging (including multiplying by r) gives a quadratic in r :

$$\frac{3}{4}(\Delta + \Gamma - 2)^2 r^2 + (\Delta + 5\Gamma - 6)r + 3 = 0, \quad (8)$$

which can be solved using the quadratic formula. After re-arranging, this gives the solution for r ,

$$r = \frac{26 - \Delta - 5\Gamma + 2\sqrt{2(\Delta - \Gamma)(3 - \Delta - 2\Gamma)}}{3(\Delta + \Gamma - 2)^2}. \quad (9)$$

From this, the spin can be determined from equation 6 and the mass by re-arranging equation 1.

Note that there is a degeneracy between pro-grade and retro-grade spin: although there are two solutions to the quadratic in r , the alternate solution with a minus sign before the determinant is a solution to the set of equations 4 and 5, but *not* to the set of equations 2 and 3; which are the equations we actually want to solve for. The solutions for mass and radius are identical with the spin being \pm the value derived assuming prograde motion. This means we can derive r , M and $|a|$ assuming prograde spin, but we do not know if the spin is prograde or retrograde. This degeneracy can be broken by measuring the highest frequency reached by the Type-C QPO: if it extends to within the ISCO for $a = -|a|$, we can assume prograde spin.

Since these solutions for r , a and M are all differentiable, it would in principle possible to apply the standard error propagation to determine uncertainties. However, these solution are non linear

functions of r , a and M , therefore the standard error propagation formula is not appropriate. Nevertheless, error estimates can be obtained through a Monte-Carlo simulation following the method outlined in M14. For each step, values for ν_{nod} , ν_{per} and ν_{ϕ} are chosen from Gaussian distributions with mean ν_{LF} , ν_{l} and ν_{u} , respectively, and standard deviation $d\nu_{\text{LF}}$, $d\nu_{\text{l}}$ and $d\nu_{\text{u}}$, respectively. Solutions for r , a and M can then be obtained analytically for each step. The mean and standard deviation for each of these three quantities then give the measurement and error. This process was very time consuming for the cases of M14 since at each step the RPM equations were solved numerically, but is very fast using the analytic formulae presented here. Of course, applying this method to the three QPOs found in GRO J1655-40, we obtained the same solution of the RPM presented in M14 (see Tab. 1).

3 SOLVING THE SYSTEM WITH TWO QPOS AND A MASS MEASUREMENT

Detection of three simultaneous QPOs is very rare for a BH. In fact, the case of GRO J1655-40 considered by M14 is so far the only reported occurrence. There are, however, detections of two simultaneous QPOs in objects which have a reliable dynamical mass measurement. This is the case for XTE J1550-564, which displays simultaneously a Type-C LF QPO and a lower HF QPO (M14a). Here, we present computationally inexpensive solutions for detections of all three possible combinations of two simultaneous QPOs coupled with a mass measurement.

3.1 ν_{per} is the unknown

In the case where we have no measurement of ν_{per} , our three unknowns are a , r and ν_{per} , while M , ν_{nod} and ν_{ϕ} are known. We can express the spin as a function of only one unknown (r) by re-arranging equation 1 to get:

$$a = \Theta \mp r^{3/2}, \quad (10)$$

where $\Theta \equiv \beta/(\nu_{\phi}M)$. Combining this with equation 5 gives:

$$3r^3 + (5 - \Delta)r^2 \mp 6\Theta r^{3/2} \mp 4\Theta r^{1/2} + 3\Theta^2 = 0. \quad (11)$$

Using the substitution $r = x^2$ leaves us with a 6th order polynomial:

$$3x^6 + (5 - \Delta)x^4 \mp 6\Theta x^3 \mp 4\Theta x + 3\Theta^2 = 0. \quad (12)$$

Unfortunately, we were unable to find an analytic solution to this equation, but since it is a polynomial, all the roots can be found using Laguerre's method. We find all six complex roots using the code ZROOTS (Press et al. 1992) and find that, for all parameter combinations trialled, there is only one real root for x (and therefore for r ; i.e. the other five roots are always complex). The spin can then be calculated from equation 10. We stress that the process of solving equation 12 using Laguerre's method is far quicker than solving the entire set of three simultaneous equations using Newton's method as in previous works.

Curiously, we find that the one real root of equation 12 is *independent* of whether we assume prograde or retrograde spin. The equation expressed using the top signs shares a common root with the equation using the bottom signs, and this happens to be the only real root. We can thus always assume prograde spin for the purposes of finding a solution for r and $|a|$ (and ν_{per}). The spin could then be $\pm|a|$ and we can again attempt to break the degeneracy by

assessing whether orbits pass inside the ISCO for the retrograde solution.

We applied this procedure to GRO J1655-40, in the two cases where a type-C QPO was detected simultaneously to a upper HF QPO (M14). We used the value of the mass obtained from spectrophotometric observations and we obtained the spin measurements reported in Table1, which are consistent with the ones reported in M14.

3.2 ν_{nod} is the unknown

By far the easiest QPO to detect is the Type-C LF QPO (Motta et al. 2012) which is associated with ν_{nod} in the RPM. However, there are some cases where the two HF QPOs are detected, but not the type-C QPO (e.g. Homan et al. 2005). Therefore, we also present the equation for r (analog to equation 12) in the case where we measure the frequency of two HF QPOs, but no LF QPO. It is derived by combining equation 10 with equation 4

$$3x^6 + (7 + \Gamma)x^4 \mp 6\Theta x^3 + 6x^2 \mp 8\Theta x + 3\Theta^2 = 0. \quad (13)$$

Similarly to the case described in Sec. 3.1, this equation can be solved using Laguerre's method to get a solution for r and $|a|$ for prograde and retrograde spin.

3.3 ν_{ϕ} is the unknown

If only a Type-C QPO and the lower HF QPO are detected (as in the case of XTE J1550-564, M14a), we cannot find an analytic solution. However, we can solve the system numerically with very little computational expense if we attempt to solve for ν_{ϕ} rather than for M .

We know ν_{nod} , ν_{per} and M . If we make a guess for ν_{ϕ} , we can then calculate a guess for r from equation 9. From this we can calculate a guess for a using equation 6 and finally calculate a guess for the mass, M_{g} , by re-arranging equation 1. The black line in Figure 1 shows the function:

$$f(\nu_{\phi}, \nu_{\text{per}}, \nu_{\text{nod}}, M) = M_{\text{g}} - M, \quad (14)$$

plotted against ν_{ϕ} , assuming $\nu_{\text{nod}} = 13.08$ Hz, $\nu_{\text{per}} = 183$ Hz and $M = 9.1$, as is the case for XTE J1550-564 (M14a). The solution for ν_{ϕ} occurs when this function crosses zero (marked by the green line). Since this is a well behaved function, it is very simple and robust to find a solution using the bisection method (we use RTBIS from Press et al. (1992) and assume $\nu_{\text{per}} < \nu_{\phi} < 1000$ Hz).

This procedure yields a solution $\nu_{\phi} = 270.5$ Hz. The radius and spin can then be determined respectively from equations 9 and 6 to give $r = 5.476$ and $a = 0.339$, consistent with the values reported by M14a (see Table 1 for error estimates).

4 PLACING LIMITS WITH TWO QPOS AND NO INDEPENDENT MASS MEASUREMENT

Even if we do not have an independent mass measurement, we can still place limits on the system by assuming that we do not see orbits inside of the ISCO, in a manner similar to Stefanov (2014). This means that the highest frequency Type-C QPO we observe must come from a radius larger than or equal to r_{ISCO} . For the case of XTE J1550-564 which has a dynamical mass measurement of $M = 9.1$, M14a showed that $r_{\text{ISCO}} = 4.83$ for their spin measurement of $a = 0.341$ and that the nodal precession frequency at r_{ISCO} for this spin and mass is $\nu_{\text{nod}}(\text{ISCO}) = 18.8$ Hz. This is encouraging

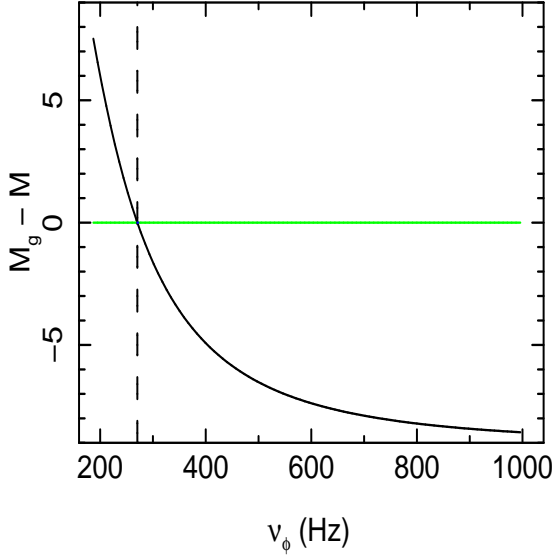


Figure 1. Function $f(\nu_\phi, \nu_{\text{per}}, \nu_{\text{nod}}, M) = M_g - M$ for the case of XTE 1550-564 (M14a), when ν_{nod} , ν_{per} and M are known. The solution for ν_ϕ corresponds to the point where this function crosses $M_g - M = 0$ (green line). This gives $\nu_\phi = 270.5$ Hz

since the highest frequency Type-C QPO ever observed from this source has a frequency $\nu_{\text{LF}}(\text{max}) = 18.04$ Hz. The data are thus consistent with the requirement of the model that $\nu_{\text{nod}}(\text{ISCO}) \geq \nu_{\text{LF}}(\text{max})$.

We can use this reasoning to place limits on the system *without* an independent mass measurement. Let us consider the case of XTE J1550-564, but say we do not have a mass measurement. We have a simultaneous measurement of ν_{nod} and ν_{per} and we also have a measurement of $\nu_{\text{LF}}(\text{max})$. We can apply the same trick as in section 3.3: we make a guess for ν_ϕ and from that calculate guesses for r , a and M using equations 9, 6 and 1. From this, we can calculate a guess for r_{ISCO} and finally a guess for $\nu_{\text{nod}}(\text{ISCO})$. In Figure 2, we plot the function:

$$f(\nu_\phi, \nu_{\text{per}}, \nu_{\text{nod}}, \nu_{\text{LF}}(\text{max})) = \nu_{\text{nod}}(\text{ISCO}) - \nu_{\text{LF}}(\text{max}), \quad (15)$$

against ν_ϕ . We can find a lower limit on ν_ϕ by determining where this function crosses zero (again, we use the bisection method). For XTE J1550-564, we find $\nu_\phi \geq 263$ Hz. From this, we can use the equations in section 2 to find $r \geq 5.39$, $a \leq 0.341$ and $M \leq 9.56$ (see Tab. 1). Since the *RXTE* monitoring of these sources was very comprehensive, it is likely that we should be able to find a Type-C QPO with $\nu_{\text{LF}}(\text{max}) \approx \nu_{\text{nod}}(\text{ISCO})$, providing a very good estimate for the system parameters. We see that the upper limit on the mass of XTE J1550-564 obtained from this method is very close to the dynamical measurement of $M = 9.1$ (Orosz et al. 2011).

4.1 The case of H1743-322

It is easy to see that this procedure will work when ν_{nod} is the unknown instead of ν_ϕ , as is the case for an observation of H1743-322 (Homan et al. 2005). We note that this is unusual, since the Type-C QPO is far easier to detect than the HF QPOs but, evidently, not impossible. In this case, the HF QPOs have frequencies $\nu_\phi = 204$ Hz and $\nu_{\text{per}} = 165$ Hz, plus the highest detected Type-C QPO

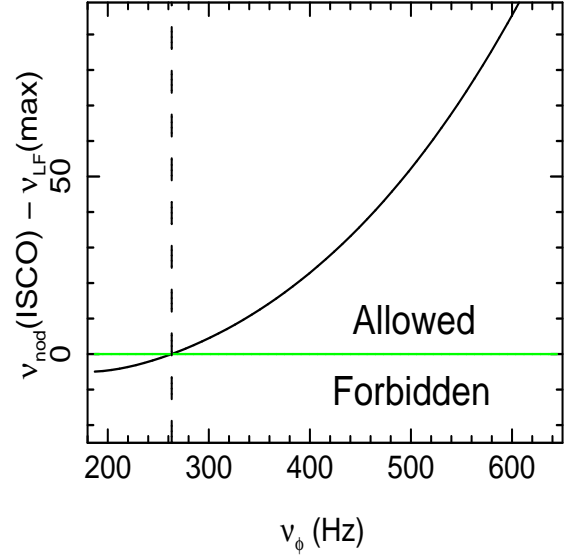


Figure 2. Function $f(\nu_\phi, \nu_{\text{per}}, \nu_{\text{nod}}, \nu_{\text{LF}}(\text{max})) = \nu_{\text{nod}}(\text{ISCO}) - \nu_{\text{LF}}(\text{max})$ for the case of XTE J1550-564, when only ν_{nod} and ν_{per} are known. The intersection between the black line and the green line (that marks $\nu_{\text{nod}}(\text{ISCO}) - \nu_{\text{LF}}(\text{max}) = 0$) corresponds to the lower limit on ν_ϕ ($\nu_\phi \geq 263$ Hz).

frequency is $\nu_{\text{LF}}(\text{max}) = 9.44$ Hz (see Table 1). We can calculate limits on M , a and r by making guesses for M . For each M trial value, we calculate the corresponding r by solving equation 13 and use this to calculate a from equation 10. From this, the ISCO can be calculated and, finally, the nodal frequency at the ISCO. In Figure 3, we plot the resulting function $f = \nu_{\text{nod}}(\text{ISCO}) - \nu_{\text{LF}}(\text{max})$ against the trial value of M . Since this function must be positive if there are to be no orbits inside the ISCO, the mass must be to the right of the dotted line. Again using a bisection search, we obtain the limits $M \geq 9.29$, $a \geq 0.21$ and $r \leq 5.89$.

In the final case where ν_{per} is the unknown frequency, limits can be placed by calculating the same function with trial values of ν_{per} and finding its root.

5 DISCUSSION & CONCLUSIONS

We have presented analytic / inexpensive numerical solutions to the RPM equations. This paper is primarily intended as a ‘cookbook’ for measuring mass and spin using the RPM and, to that end, we have written a user friendly FORTRAN code which finds solutions, with error estimates, for any of the cases mentioned here. Any interested readers wishing to use this code are encouraged to contact us.

For the case when three simultaneous QPOs are observed, we have found analytical solutions to derive the mass and spin of the black hole. For the case when only two QPOs are detected simultaneously, a dynamical mass measurement can be combined with the QPO frequencies to provide a spin measurement. Even when no dynamical mass measurement exists, we can still place limits on the spin of the black hole by requiring that the highest Type-C QPO frequency ever observed from the source must come from an orbit larger than or coincident to the ISCO.

We note that, in principle, we could also solve for mass with two simultaneously detected QPOs and a measurement of spin via spectroscopic methods (i.e. fitting the disk spectrum or iron line

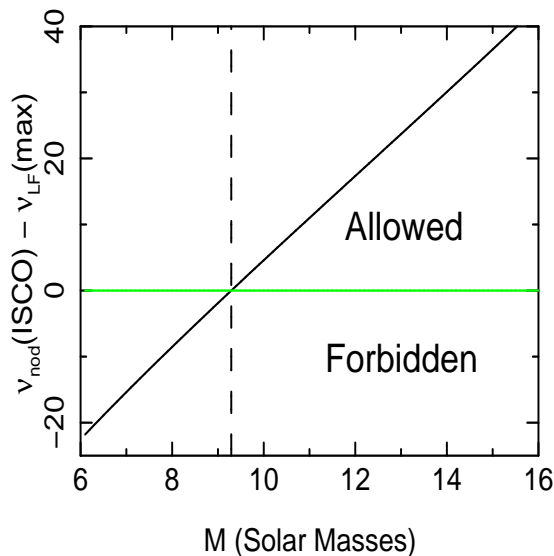


Figure 3. Function $f(\nu_\phi, \nu_{\text{per}}, \nu_{\text{nod}}, \nu_{\text{LF(max)}}) = \nu_{\text{nod}}(\text{ISCO}) - \nu_{\text{LF(max)}}$ for the case of H 1743-322, when only ν_ϕ and ν_{per} are known. The intersection between the black line and the green line (that marks $\nu_{\text{nod}}(\text{ISCO}) - \nu_{\text{LF(max)}} = 0$) corresponds to the lower limit on M ($M \geq 9.29$).

profile; Kolehmainen & Done 2010; Fabian et al. 2012). However, the large uncertainties associated with the spin, particularly after comparison between the disk and iron line estimates, limit the usefulness of this exercise.

We note that the RPM simply considers test mass orbits in the Kerr metric. Further theoretical framework is required to understand exactly how these frequencies will modulate the X-ray flux from an accretion flow, which comprises an optically thick, geometrically thin accretion disk (e.g. Shakura & Sunyaev 1973) and some optically thin electron cloud emitting a Comptonised power law spectrum (Thorne & Price 1975). The LF QPO model of Ingram et al. (2009) considers a truncated disk / inner hot flow geometry in which nodal precession of the entire inner flow results from the frame dragging effect. This naturally explains how the precession frequency modulates the X-ray flux (Ingram & Done 2012; Veledina et al. 2013) and how a coherent LF QPO can be observed even when the inner flow is thought to be rather extended. The HF QPOs, on the other hand, are only observed with high frequencies, when the disk truncation radius is thought to be close to the ISCO. We do, however, see broad power spectral features with characteristic frequencies that co-evolve with the LF QPO frequency and appear to eventually evolve into HF QPOs (Psaltis et al. 1999). M14 and M14a used their spin and mass constraints for GRO 1655-40 and XTE J1550-564 respectively to demonstrate that this co-evolution is roughly consistent with the high frequency features peaking at ν_{per} and ν_ϕ and the LF QPO peaking at ν_{nod} , all for a moving radius.

Thus, perhaps the periastron precession and orbital frequencies modulate the X-ray flux through randomly occurring anisotropies in the inner accretion flow (see e.g. Wellons et al. 2014; Schnittman et al. 2006). Bakala et al. (2014) demonstrate that HF QPOs at the epicyclic frequencies are seen from X-ray emitting blobs orbiting a BH, resulting mainly from variable Doppler effects. When the inner flow is extended (and assuming

that modulations from different radii are not correlated; see e.g. Ingram & van der Klis 2013), there will be modulations at a large range of frequencies, resulting in broad power spectral features. When the truncation radius is close to the ISCO, this picture converges to the RPM in which the anisotropies only occur for a thin ring, and so we see QPOs at three frequencies. We will develop a formalism for this model in a future paper in order to test it against the observed co-evolution of the broad high frequency features and the LF QPO.

For the simultaneously detected QPOs considered here, there are two objects for which we are able to make multiple spin measurements. For GRO 1655-40, we obtain 3 spin estimates which are all consistent with one another. For XTE J1550-564, we obtain an upper limit of $a \leq 0.341$, consistent with the measurement of $a = 0.339 \pm 0.007$ presented here and in M14a. This is encouraging, and we note that the *Large Observatory For x-ray Timing (LOFT)*; Feroci & LOFT Consortium 2011), should it fly, will detect many more triplets of HF QPOs to test the RPM more thoroughly.

ACKNOWLEDGMENTS

AI and SEM acknowledge the Observatory of Rome for hospitality. SEM acknowledges support from the ESA research fellowship program.

REFERENCES

- Abramowicz M. A., Kluźniak W., 2001, *A&A*, 374, L19
- Altamirano D., Ingram A., van der Klis M., Wijnands R., Linares M., Homan J., 2012, *ApJ*, 759, L20
- Bakala P., Török G., Karas V., Dovčiak M., Wildner M., Wzientek D., Šrámková E., Abramowicz M., Goluchová K., Mazur G. P., Vincent F. H., 2014, *MNRAS*, 439, 1933
- Bambi C., Malafarina D., Tsukamoto N., 2014, *ArXiv e-prints*
- Bardeen J. M., Press W. H., Teukolsky S. A., 1972, *ApJ*, 178, 347
- Beer M. E., Podsiadlowski P., 2002, *MNRAS*, 331, 351
- Belloni T. M., Motta S. E., Muñoz-Darias T., 2011, *Bulletin of the Astronomical Society of India*, 39, 409
- Cabanac C., Henri G., Petrucci P.-O., Malzac J., Ferreira J., Belloni T. M., 2010, *MNRAS*, 404, 738
- Casella P., Belloni T., Stella L., 2005, *ApJ*, 629, 403
- Fabian A. C., Wilkins D. R., Miller J. M., Reis R. C., Reynolds C. S., Cackett E. M., Nowak M. A., Pooley G. G., Pottschmidt K., Sanders J. S., Ross R. R., Wilms J., 2012, *MNRAS*, 424, 217
- Feroci M., LOFT Consortium t., 2011, *ArXiv e-prints*
- Fragile P. C., Miller W. A., Vandernoot E., 2005, *ApJ*, 635, 157
- Gierliński M., Middleton M., Ward M., Done C., 2008, *Nature*, 455, 369
- Homan J., Buxton M., Markoff S., Bailyn C. D., Nespoli E., Belloni T., 2005, *ApJ*, 624, 295
- Homan J., Wijnands R., Kong A., Miller J. M., Rossi S., Belloni T., Lewin W. H. G., 2006, *MNRAS*, 366, 235
- Ingram A., Done C., 2010, *MNRAS*, 405, 2447
- Ingram A., Done C., 2011, *MNRAS*, 415, 2323
- Ingram A., Done C., 2012, *MNRAS*, 427, 934
- Ingram A., Done C., Fragile P. C., 2009, *MNRAS*, 397, L101
- Ingram A., van der Klis M. v. d., 2013, *MNRAS*, 434, 1476
- Kluźniak W., Abramowicz M. A., 2001, *ArXiv Astrophysics e-prints*

- Kolehmainen M., Done C., 2010, MNRAS, 406, 2206
Lamb F. K., Miller M. C., 2001, ApJ, 554, 1210
Merloni A., Vietri M., Stella L., Bini D., 1999, MNRAS, 304, 155
Motta S., Homan J., Muñoz Darias T., Casella P., Belloni T. M., Hiemstra B., Méndez M., 2012, MNRAS, 427, 595
Motta S. E., Belloni T. M., Stella L., Muñoz-Darias T., Fender R., 2014, MNRAS, 437, 2554
Motta S. E., Muñoz-Darias T., Sanna A., Fender R., Belloni T., Stella L., 2014, MNRAS
Orosz J. A., Steiner J. F., McClintock J. E., Torres M. A. P., Remillard R. A., Bailyn C. D., Miller J. M., 2011, ApJ, 730, 75
Press W. H., Teukolsky S. A., Vetterling W. T., Flannery B. P., 1992, Numerical recipes in FORTRAN. The art of scientific computing. Cambridge: University Press, —c1992, 2nd ed.
Psaltis D., Belloni T., van der Klis M., 1999, ApJ, 520, 262
Schnittman J. D., Homan J., Miller J. M., 2006, ApJ, 642, 420
Shakura N. I., Sunyaev R. A., 1973, A&A, 24, 337
Stefanov I. Z., 2014, ArXiv e-prints
Stella L., Vietri M., 1998, ApJ, 492, L59+
Stella L., Vietri M., 1999, Physical Review Letters, 82, 17
Stella L., Vietri M., Morsink S. M., 1999, ApJ, 524, L63
Strohmayer T. E., Markwardt C. B., Swank J. H., in't Zand J., 2003, ApJ, 596, L67
Tagger M., Pellat R., 1999, A&A, 349, 1003
Thorne K. S., Price R. H., 1975, ApJ, 195, L101
Titarchuk L., Osherovich V., 1999, ApJ, 518, L95
van der Klis M., 1996, in van Paradijs J., van den Heuvel E. P. J., Kuulkers E., eds, Compact Stars in Binaries Vol. 165 of IAU Symposium, Low-Mass X-ray Binaries - Recent Developments. p. 301
Veledina A., Poutanen J., Ingram A., 2013, ApJ, 778, 165
Wagoner R. V., Silbergleit A. S., Ortega-Rodríguez M., 2001, ApJ, 559, L25
Wellons S., Zhu Y., Psaltis D., Narayan R., McClintock J. E., 2014, ApJ, 785, 142
Wijnands R., Homan J., van der Klis M., 1999, ApJ, 526, L33

Table 1: Solutions of the RPM obtained through the analytical and semi-analytical methods presented in this work. The frequencies have been taken from the literature.

	Type-C	Lower HF QPO	Upper HF QPO	Mass	Ref.	Solutions		
	Frequency [Hz]	Frequency [Hz]	Frequency [Hz]			Mass	Spin	Radius
GRO J1655-40								
3 QPOs	$17.3^{+0.1}_{-0.1}$	298^{+4}_{-4}	441^{+2}_{-2}	$5.4 \pm 0.3 M_{\odot}$	(1)	$5.31 \pm 0.07 M_{\odot}$	0.285 ± 0.003	5.68 ± 0.04
2 QPOs and mass	$18.3^{+0.1}_{-0.1}$		451^{+6}_{-5}		(1, 2)		0.28 ± 0.02	5.5 ± 0.2
2 QPOs and mass	$18.1^{+0.1}_{-0.1}$		446^{+4}_{-4}				0.29 ± 0.02	5.6 ± 0.2
XTE J1550-564								
2 QPOs and mass	13.08 ± 0.08	183 ± 5		$9.10 \pm 0.61 M_{\odot}$	(3, 4)		0.339 ± 0.007	5.47 ± 0.12
2 QPOs	13.08 ± 0.08	183 ± 5			(3)	$\leq 9.56 M_{\odot}$	≤ 0.341	≥ 5.39
	highest detected: 18.04 ± 0.07							
H1743-322								
2 QPOs	highest detected: 9.44 ± 0.02	165^{+9}_{-5}	240 ± 3		(5)	$\geq 9.29 M_{\odot}$	≥ 0.21	≤ 5.89

REFERENCES: (1) Motta et al. (2014); (2) Beer & Podsiadlowski (2002) (3) Motta et al. (2014); (4) Orosz et al. (2011); (5) Homan et al. (2005).